THE JOURNAL OF PHYSICAL CHEMISTRY B

Article

pubs.acs.org/JPCB

Water Exchange Rates and Molecular Mechanism around Aqueous Halide Ions

Harsha V. R. Annapureddy and Liem X. Dang*

Physical Sciences Division, Pacific Northwest National Laboratory, Richland, Washington 93352, United States

Supporting Information

ABSTRACT: Molecular dynamics simulations were performed to systematically study the water-exchange mechanism around aqueous chloride, bromide, and iodide ions. Transition state theory, Grote−Hynes theory, and the reactive flux method were employed to compute water exchange rates. We computed the pressure dependence of rate constants and the corresponding activation volumes to investigate the mechanism of the solvent exchange event. The activation volumes obtained using the transition state theory rate constants are negative for all the three anions, thus indicating an associative mechanism. Contrary to the transition state theory results, activation volumes obtained using rate constants from Grote−Hynes theory and the reactive flux method are positive, thus indicating a dissociative mechanism.

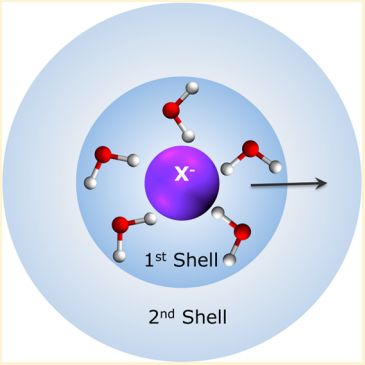

1. INTRODUCTION

Ion solvation has received much attention over recent decades because solvated ions play an important role in many chemical and biological processes. Knowledge of the role and importance of solvated ions has grown; however, continued advancement of our fundamental understanding of solvated ions and the mechanism of the processes involved in solvation is crucial. The primary focus of this article is to use computational techniques to understand the solvent-exchange process in aqueous halide solutions. Replacement of a solvent molecule from the first coordination shell is an important step in the reactivity of ions in solutions and also a key step for the ion recognition in biological systems. The rates and mechanism of exchange greatly depend on the type of ion and its charge.[1] A simple solvent exchange reaction can be represented as shown below.

$$[\mathrm{I(solvent)}_n]^z + \mathrm{solvent}^* \rightleftharpoons [\mathrm{I(solvent)}_{n-1}(\mathrm{solvent}^*)]^z + \mathrm{solvent}$$

Here, "I" represents the ion with "n" number of solvent molecules in the first coordination shell, and "solvent*" represents the incoming solvent molecule. In this reaction, we note that the reactants and products are identical; in addition, incoming and outgoing solvent molecules are similar. This makes studying solvent exchange rates and mechanisms through experiments a challenge. Computational techniques such as molecular dynamics (MD) simulations can provide more insight and molecular details of the processes involved in the solvent-exchange process.

Solvent-exchange mechanisms are broadly classified into two categories on the basis of the position of the incoming and outgoing solvent molecules relative to the ion; namely, (1) associative and (2) dissociative mechanisms.[1−3] In an associative mechanism, both the incoming and outgoing solvent molecules are considerably coordinated with the ion at the transition state. In a dissociative mechanism, the incoming and outgoing solvent molecules are not significantly coordinated with the ion at the transition state. These mechanisms are similar to substitution reactions in organic chemistry. The associative mechanism is similar to substitution reaction SN2, whereas the dissociative mechanism is similar to substitution reaction SN1. The key parameter to assign to mechanisms for the solvent exchange reaction is the activation volume ($\Delta V^{\ddagger}$), which is defined as the difference between the partial molar volume of the reactants and the transition state. If the value of $\Delta V^{\ddagger}$ is negative, the solvent exchange mechanism is associative; if the value of $\Delta V^{\ddagger}$ is positive, then the exchange mechanism is dissociative. Activation volume is determined using the pressure dependence of the rate constants.

Several experimental[1,2,4,5] and simulation studies[6−13] have been performed to understand the exchange mechanisms involved in the aqueous solutions of alkali and alkaline earth metals. Hynes et al. studied the water exchange rates and mechanism of aqueous Li^+ and Na^+ at normal temperature and pressure using nonpolarizable force fields.[9,10] Rustad et al. performed pressure-dependence studies on rate constants using MD simulations to understand the solvent exchange mechanism in aqueous Li^+ solutions.[12] Most previous studies on solvent-exchange mechanisms focused only on cations; much less is known regarding solvent exchange process around anions.

Special Issue: James L. Skinner Festschrift

Received: January 14, 2014
Revised: February 22, 2014
Published: March 6, 2014

Our main motivation for this work was to develop a molecular model that describes the thermodynamic and kinetic properties of the water exchange process around aqueous halide ions. We first computed free energy profiles using the constrained mean force approach, taking into account polarization effects. Next, we estimated the rate constants using transition state theory (TST) and then estimated transmission coefficients using Grote−Hynes (GH) theory and the reactive flux (RF) method. Finally, through the pressure dependence of the rate constants, we evaluated the activation volumes for chloride, bromide, and iodide ions. The remainder of this paper is organized as follows. In Section 2, the potential models and simulation methods are described. The results and discussion are presented in Section 3, and the conclusions are discussed in Section 4.

2. METHODS

Our MD simulations were performed using a modified version of the Amber 9 package.[14] Polarizable force-field parameters used for halide ions and water were those previously developed in our group.[15,16] Simulation boxes consisted of a single ion solvated with 1000 water molecules. For all three ions, equilibration runs of 10 ns were carried out in an NPT ensemble at 300 K temperature and at pressures of 0, 100, and 200 MPa. The final configurations obtained from the equilibration runs were used to perform constrained MD simulations. Using constrained MD simulations[17,18] and eq 1, we evaluated the potential of mean force (PMF) along the center-of-mass separation between the ion and one of the chosen water molecules.

$$F(r) = \frac{1}{2}\langle \hat{r}_{com}\cdot(\vec{F}_2 - \vec{F}_1)\rangle \tag{1}$$

In eq 1, $\vec{F}_1$ and $\vec{F}_2$ are the forces acting on the ion and the chosen water molecule. The term $\vec{r}_{com}$ is the unit vector along the center-of-mass separation between the ion and the water molecule, and $\langle ...\rangle$ represents the average over several configurations.

We carried out a series of MD simulations at various center-of-mass separation distances with increments of 0.125 Å. In each of these MD simulations, the center-of-mass separation between the ion and the chosen water molecule was fixed, and the solvent configurations were sampled to evaluate the mean force, $F(r)$, using eq 1. At each distance, $F(r)$ was obtained through an average over 4 ns of simulation. At higher pressures, to obtain better convergence, the value of $F(r)$ was obtained by computing an average over 8 ns of constrained simulations. All of these simulations were performed in an NVT ensemble at 300 K. Using these $F(r)$ values and eq 2, we computed PMFs for chloride, bromide, and iodide at three different pressures: 0, 100, and 200 MPa.

$$W(r) = -\int_{r_0}^{r} F(r)\, dr \tag{2}$$

We performed the MD simulations using the periodic boundary conditions on all three directions with a time step of 2 fs. We used the Ewald summation technique to handle long-range electrostatic interactions,[19] and the SHAKE algorithm was employed in the simulations to fix the internal geometry of water.[20]

We computed the rate constants using TST, GH theory, and the RF method.

$$k^{TST} = \frac{1}{\sqrt{2\pi\mu\beta}} \frac{(r^*)^2 e^{-\beta W(r^*)}}{\int_0^{r^*} r^2 e^{-\beta W(r)}\, dr} \tag{3}$$

Using the computed PMFs and eq 3, we estimated TST rate constants (k^{TST}).[21−23] In eq 3, r^* is defined as the position of the barrier top, μ is the ion−water reduced mass, and $\beta = 1/k_bT$. Because TST does not account for recrossings due to solvent dynamics, we used GH theory and the RF method. Both of these methods correct the TST rate constant through a transmission coefficient, κ, that gives the probability that the activated species will reach the products. The corrected rate constant is given by κk^{TST}. The term κ takes values between zero and unity.

$$\kappa_{GH} = \left(\kappa_{GH} + \int_0^{\infty} dt\, \frac{\zeta(t)}{\omega_b} e^{-\omega_b \kappa_{GH} t}\right)^{-1} \tag{4}$$

The transmission coefficient from GH theory, κ_{GH}, is determined by iteratively solving eq 4. In this equation, $\zeta(t)$ is the time dependent friction on the reaction coordinate. The barrier frequency, ω_b, is obtained using a parabolic approximation to the PMF at the barrier region. According to GH theory, the transmission coefficient depends on the Laplace transform of the time-dependent friction at frequency $\omega_b\kappa_{GH}$. Readers can refer to the literature for more details on GH theory.[22,24,25]

According to the RF method, the transmission coefficient, κ_{RF}, is extracted from the plateau value of the time-dependent transmission, $\kappa(t)$, which we computed using eq 5.[26,27]

$$\kappa(t) = \frac{\langle \dot{r}(0)\, \theta[r(t) - r^*]\, \delta(r - r^*)\rangle}{\langle \dot{r}(0)\, \theta[\dot{r}(0)]\, \delta(r - r^*)\rangle} \tag{5}$$

here, $\dot{r}(0)$ is the initial ion−water velocity along the reaction coordinate, and $\theta(x)$ is a Heaviside function, which is 1 if $x > 0$ and 0 otherwise.

To compute $\kappa(t)$, we generated a series of initial configurations with the reaction coordinate fixed at the transition state. To obtain these configurations, we ran a 20-ns simulation in a constrained reaction coordinate ensemble. Coordinates are saved every 8 ps to obtain 2500 configurations. Using these initial configurations and initial velocities sampled though a Boltzmann distribution; we propagated trajectories both forward and backward in time for 2 ps. The value of κ_{RF} was extracted by taking the average over the last 0.5 ps of $\kappa(t)$.

3. RESULTS AND DISCUSSION

We first discuss the water exchange rates computed using various rate theories and its pressure dependence for one anion (chloride), then we compare and discuss the results obtained for different anions. In Figure 1, we show the computed PMFs for a chloride−water pair at three different pressures: 0, 100, and 200 MPa. It is clearly evident from this plot that the barrier heights decrease as pressure increases. Rustad et al.[12] and Dang et al.[7] also reported similar trends in the barrier heights in their water exchange studies on Li^+. This decrease in barrier heights results in an increase in the TST rate constants (κ^{TST}) with pressure. The barrier height at 0 MPa is ∼1 kcal/mol, which is close to barrier heights observed in previous studies by Hynes et al. for polarizable models.[28]

To understand the mechanism of solvent exchange, we determined the activation volume using the pressure dependence of rate constants and eqs 6 and 7.

dx.doi.org/10.1021/jp500402j | J. Phys. Chem. B 2014, 118, 7886−7891

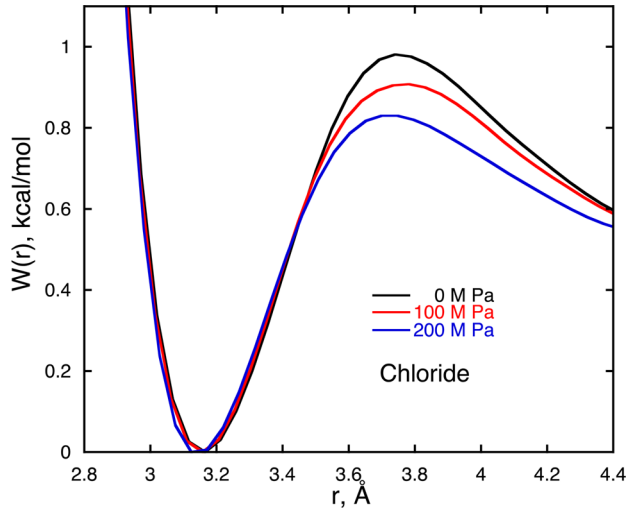

Figure 1. Pressure dependence of the PMF, $W(r)$ of Cl^-−H_2O systems.

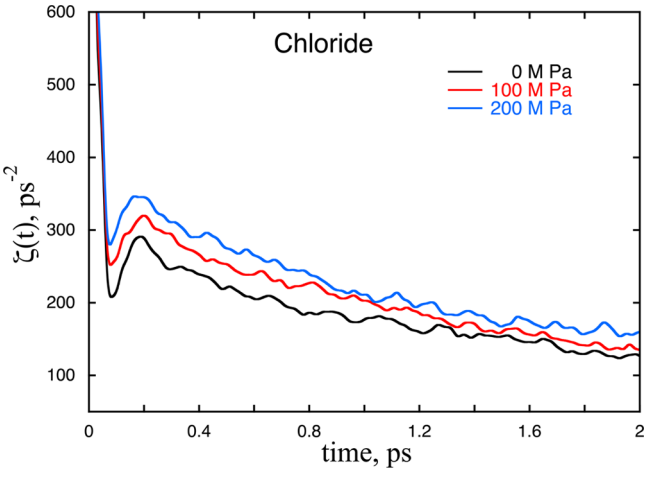

Figure 2. Pressure dependence of the time dependence friction kernels, $\zeta(t)$, of Cl^-−H_2O systems.

Table 1. Rate Theory Results[a]

	pressure, MPa	k^{TST}, ps^{-1}	κ_{GH}	κ_{RF}
chloride	0	1.07	0.043	0.10
	100	1.20	0.027	0.04
	200	1.32	0.018	0.02
bromide	0	1.22	0.034	0.09
	100	1.33	0.025	0.05
	200	1.46	0.020	0.04
iodide	0	1.52	0.035	0.09
	100	1.64	0.028	0.05
	200	1.78	0.020	0.04

[a]The estimated error in transmission coefficients is ±0.01.

$$\Delta V^{\ddagger} = -RT\left(\frac{\partial \ln(k)}{\partial P}\right)_T \tag{6}$$

$$\ln\left(\frac{k_p}{k_0}\right) = -\Delta V^{\ddagger}\frac{P}{RT} \tag{7}$$

Here, R is the gas constant, T is temperature, P is pressure, k is the rate constant, and $\Delta V^{\ddagger}$ is the activation volume. Equation 7 is a linear approximation to the eq 6. Here, k_p and k_0 are the rate constants at pressure P and 0, respectively. The computed rate constants at different pressures are substituted into eq 7 to obtain the activation volume. The value of $\Delta V^{\ddagger}$ obtained from

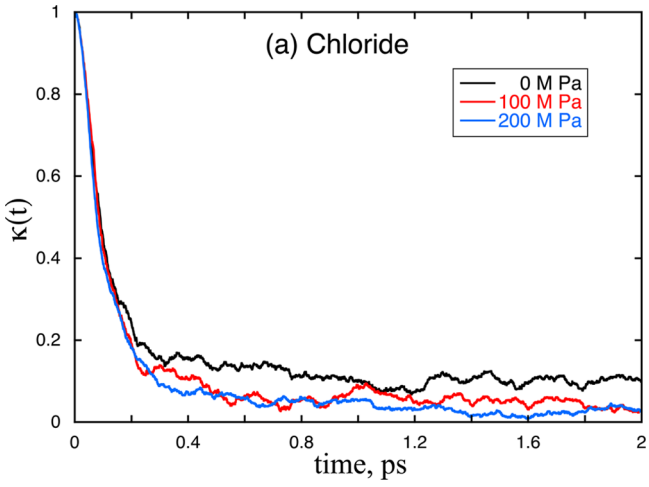

Figure 3. Pressure dependence of the transmission coefficients, $k(t)$, of Cl^-−H_2O systems.

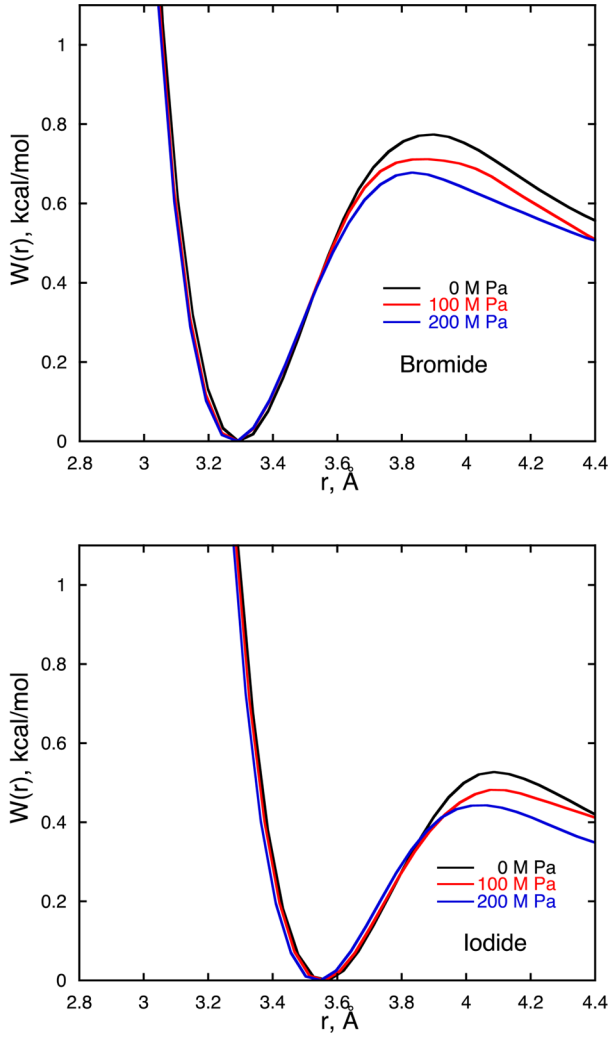

Figure 4. Pressure dependence of the PMF, $W(r)$ of Br^-−H_2O and I^-−H_2O systems.

dx.doi.org/10.1021/jp500402j | J. Phys. Chem. B 2014, 118, 7886−7891

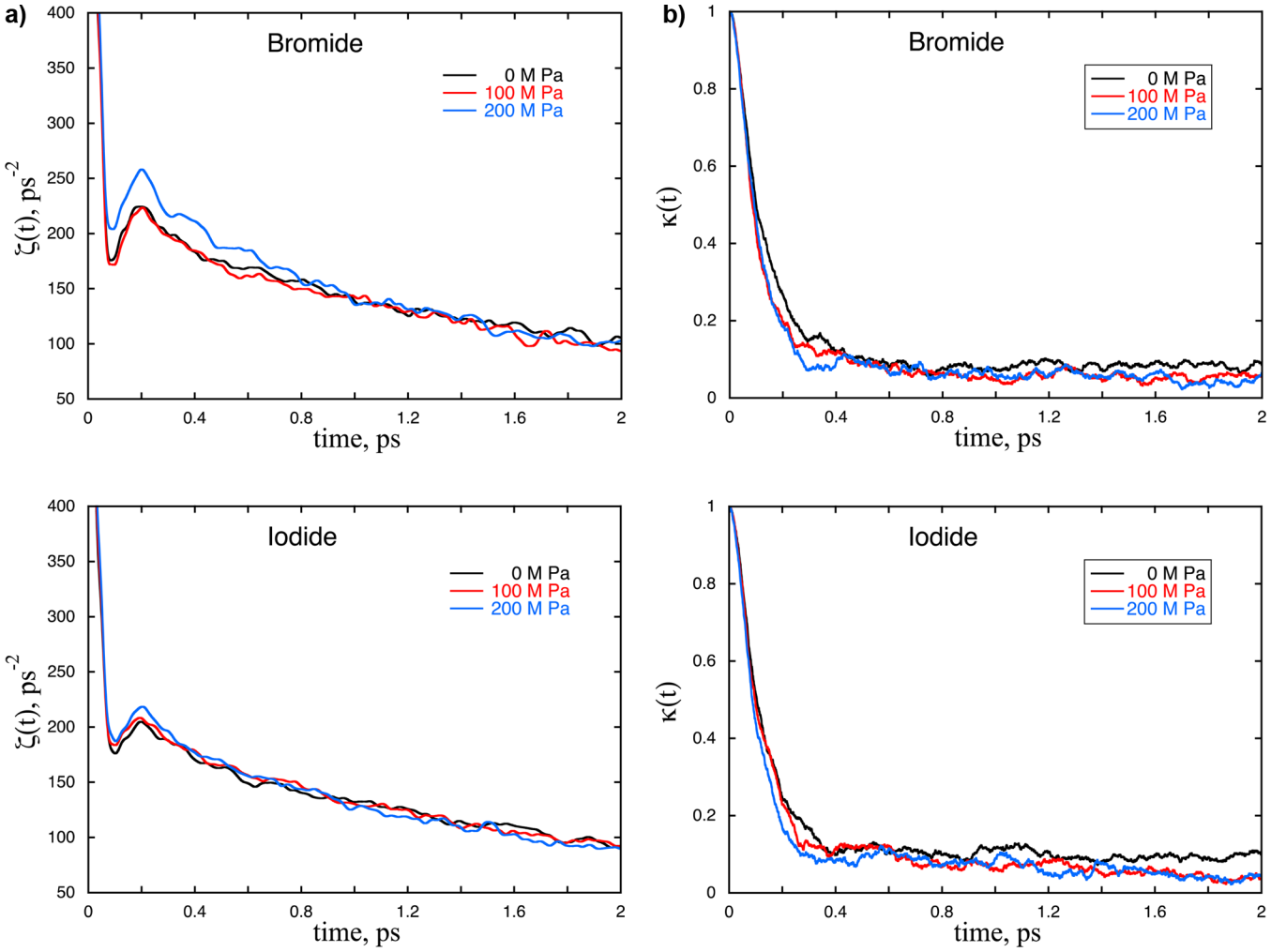

Figure 5. (a) Pressure dependence of the time dependence friction kernels, $\zeta(t)$, of Br^--H_2O (top) and I^--H_2O (bottom) systems. (b) Pressure dependence of the transmission coefficients, $k(t)$, of Br^--H_2O (top) and I^--H_2O (bottom) systems.

TST rate constants is −2.66 cm^3/mol. A full detailed synopsis of how we computed the activation volumes is given in the Supporting Information. This is slightly negative, thus indicating an associative mechanism for the water-exchange process around the chloride ion.

In Figure 2, we show friction kernels, $\zeta(t)$, for chloride cases at various pressures. In all cases, the friction kernels exhibit similar profiles with two distinct decay time scales: an initial fast subpicosecond decay followed by a longer time decay that lasts for few picoseconds. Barrier frequencies also decrease as pressure increases. Using the time-dependent friction along the reaction coordinate and the barrier frequency, we computed the GH theory transmission coefficients, and the results are presented in Table 1. The transmission coefficient, κ_{GH}, for chloride at 0 MPa is 0.04. This is a very small value and indicates a large number of recrossing events that are induced by solvent friction. The pressure dependence of transmission coefficients is shown in Table 1. As pressure increases, transmission coefficients, κ_{GH}, decrease.

In Figure 3, we show the time-dependent transmission, $\kappa(t)$, computed using the RF method. We calculated the transmission coefficient, κ_{RF}, by taking the average over last 0.5 ps of $\kappa(t)$. From values listed in Table 1, we see that κ_{RF} decreases as pressure increases. Both GH theory and the RF method yield similar trends in pressure dependence of the transmission coefficients. The computed activation volumes from GH theory and the RF method are 8.4 and 15.8 cm^3/mol, respectively. Contrary to the TST result, the activation volumes from the GH and RF methods are positive, thus indicating a dissociative mechanism. Therefore, just considering the TST rates does not provide the correct mechanism for solvent exchange. One needs to be careful with systems in which solvent dynamics plays an important role. Previous studies by our group and also by Rustad et al. found that transmission coefficients increase with an increase in pressure for Li^+. Contrary to these observations, we observed an opposite trend for the chloride ion. This implies that the pressure dependence of the transmission coefficient does not follow a universal trend and greatly depends on the ion and its charge.

In Figure 4, we show the computed PMFs for all the bromide−water and iodide−water pairs at three different pressures: 0, 100, and 200 MPa. The first observation upon comparing the PMFs of all three ions is that the barrier height decreases from chloride to iodide with the increase in anion size. This behavior is expected because the chloride ion has stronger interactions with water compared with the other two ions. In addition, similar to the chloride case, bromide and iodide ions show a decrease in barrier height with the increase in pressure. The decrease in barrier height is 0.15 kcal/mol for chloride, 0.1 kcal/mol for bromide, and 0.09 kcal/mol for iodide. From these values, we

dx.doi.org/10.1021/jp500402j | J. Phys. Chem. B 2014, 118, 7886−7891

noticed that the effect of pressure on the barrier height decreases from chloride to iodide with the increase in ion size. The pressure dependence of the barrier height is more prominent for chloride and decreases with the increase in ion size. In addition, as expected with the increase in pressure, there is a slight left shift in the barrier height position. The values for k^{TST} reported in Table 1 clearly show that the water-exchange rate from the first solvation shell to the second solvation shell increases as pressure increases for all three ion cases. This is a direct consequence of the trend in barrier heights.

In Figure 5, we show the friction kernels for bromide and iodide cases. Similar to the chloride case discussed earlier, the friction kernels for bromide and iodide also exhibit two distinct time scales of decay. The computed transmission coefficients in Table 1 clearly show decreases as pressure increases for all the anions. In Figure 5, we show the time-dependent transmission coefficients determined using the RF method for the rest of the anions at different pressures. The corresponding transmission coefficients, κ_{RF}, reported in Table 1 also decrease as pressure increases. The computed rate constants using GH theory and the RF method for the bromide and iodide cases decrease as pressure increases. This trend is similar to the chloride case, as discussed earlier. The activation volumes computed using rate constants from various theories are presented in Table 2. For all the anions, the activation volumes obtained from TST are negative, thus indicating an associative water-exchange mechanism, whereas taking into account the dynamical effects of the solvent using GH theory and the RF method gives positive activation volumes that indicate a dissociative mechanism for all the anions. This result emphasizes the importance of dynamical effects in determining the rates and mechanism of the solvent exchange process. In addition, the pressure dependence of transmission coefficients significantly contributes to the activation volume.

Table 2. Activation Volumes Computed from Various Rate Theories

	transition state theory, $\Delta V^{\ddagger}$, cm^3/mol	Grote–Hynes theory, $\Delta V^{\ddagger}$, cm^3/mol	reactive flux method, $\Delta V^{\ddagger}$, cm^3/mol
chloride	−3 ± 2	8 ± 2	16 ± 2
bromide	−2 ± 2	4 ± 2	7 ± 2
iodide	−2 ± 2	4 ± 2	9 ± 2

The residence times, τ, for water in the aqueous chloride, bromide, and iodide ions obtained from the RF method are shown in Table 3. For comparison, we also show residence times previously reported by Koneshan et al.[29] The slight differences in residence times can be attributed to the difference in potential models used in the studies. In addition, residence times reported by Koneshan et al. were computed using a different method given by Impey et al.[30]

Table 3. Residence Times, $\tau = 1/\kappa_{RF}k^{TST}$ [a]

		residence time, ps	
	pressure, MPa	RF	Koneshan et al.
chloride	0	9	16.6
	100	19	
	200	31	
bromide	0	9	13.2
	100	14	
	200	15	
iodide	0	7	13.8
	100	13	
	200	13	

[a]The estimated error in computed residence times is ±2 ps.

4. CONCLUSIONS

Through MD simulations using polarizable force filed models, we studied in detail the water-exchange mechanism around the aqueous halide ions. We computed the PMFs and estimated rate constants using three different rate theories: TST, GH theory, and the RF method. We investigated the pressure dependence of rate constants to understand the water-exchange mechanism from the first solvation shell. Our results show that, for all the anions, barrier heights decrease as pressure increases, and as a result, the TST rate constants increase as pressure increases. Transmission coefficients computed using GH theory and the RF method decrease as pressure increases. Rate constants calculated using GH theory and the RF method decrease as pressure increases. The activation volume, which is a key indicator of the exchange mechanism, was found to be negative from TST, indicating an associative mechanism for all the anions. Contrary to this finding, calculations using GH theory and the RF method yield positive activation volumes, thus indicating a dissociative mechanism for all the anions.

■ ASSOCIATED CONTENT

Supporting Information

Calculations; transition state theory, reactive flux method, Grote–Hynes theory graphs, This information is available free of charge via the Internet at http://pubs.acs.org

■ AUTHOR INFORMATION

Corresponding Author

*Phone: (509) 375-2557. E-mail: liem.dang@pnnl.gov.

Notes

The authors declare no competing financial interest.

■ ACKNOWLEDGMENTS

The Division of Chemical Sciences, Geosciences, and Biosciences, Office of Basic Energy Sciences (BES), of the U.S. Department of Energy (DOE) funded this work. Battelle operates Pacific Northwest National Laboratory for DOE. The calculations were carried out using computer resources provided by BES.

■ REFERENCES

(1) Helm, L.; Merbach, A. E. Inorganic and bioinorganic solvent exchange mechanisms. *Chem. Rev.* **2005**, *105* (6), 1923–1959.
(2) Helm, L.; Merbach, A. E. Water exchange on metal ions: experiments and simulations. *Coord. Chem. Rev.* **1999**, *187*, 151–181.
(3) Rotzinger, F. P. Treatment of substitution and rearrangement mechanisms of transition metal complexes with quantum chemical methods. *Chem. Rev.* **2005**, *105* (6), 2003–2037.
(4) Buchner, R.; Chen, T.; Hefter, G. Complexity in "simple" electrolyte solutions: Ion pairing in $MgSO_4$(aq). *J. Phys. Chem. B* **2004**, *108* (7), 2365–2375.
(5) Buchner, R. What can be learnt from dielectric relaxation spectroscopy about ion solvation and association? *Pure Appl. Chem.* **2008**, *80* (6), 1239–1252.
(6) Loeffler, H. H.; Inada, Y.; Funahashi, S. Water exchange dynamics of lithium(I) ion in aqueous solution. *J. Phys. Chem. B* **2006**, *110* (11), 5690–5696.

(7) Dang, L. X.; Annapureddy, H. V. R. Computational studies of water exchange around aqueous Li^+ with polarizable potential models. *J. Chem. Phys.* **2013**, *139* (8), 084506.
(8) Rey, R.; Hynes, J. T. Hydration shell exchange dynamics for Na^+ in water. *J. Phys.: Condens. Matter* **1996**, *8* (47), 9411−9416.
(9) Rey, R.; Hynes, J. T. Hydration shell exchange kinetics: An MD study for Na^+(aq). *J. Phys. Chem.* **1996**, *100* (14), 5611−5615.
(10) Spangberg, D.; Rey, R.; Hynes, J. T.; Hermansson, K. Rate and mechanisms for water exchange around Li^+(aq) from MD simulations. *J. Phys. Chem. B* **2003**, *107* (18), 4470−4477.
(11) Casey, W. H. Large aqueous aluminum hydroxide molecules. *Chem. Rev.* **2006**, *106*, 1−16.
(12) Rustad, J. R.; Stack, A. G. Molecular dynamics calculation of the activation volume for water exchange on Li^+. *J. Am. Chem. Soc.* **2006**, *128* (46), 14778−14779.
(13) Kerisit, S.; Rosso, K. M. Transition path sampling of water exchange rates and mechanisms around aqueous ions. *J. Chem. Phys.* **2009**, *131* (11), 114512.
(14) Case, D. A.; Darden, T. A.; Cheatham, T. E., III; Simmerling, C. L.; Wang, J.; Duke, R. E.; Luo, R.; Merz, K. M.; Pearlman, D. A.; Crowley, M.; Walker, R. C.; Zhang, W.; Wang, B.; Hayik, S.; Roitberg, A.; Seabra, G.; Wong, K. F.; Paesani, F.; Wu, X.; Brozell, S.; Tsui, V.; Gohlke, H.; Yang, L.; Tan, C.; Mongan, J.; Hornak, V.; Cui, G.; Beroza, P.; Mathews, D. H.; Schafmeister, C.; Ross, W. S.; Kollman, P. A. *AMBER 9*; University of California: San Francisco, 2006.
(15) Dang, L. X.; Chang, T. M. Molecular dynamics study of water clusters, liquid, and liquid-vapor interface of water with many-body potentials. *J. Chem. Phys.* **1997**, *106* (19), 8149−8159.
(16) Dang, L. X. Computational study of ion binding to the liquid interface of water. *J. Phys. Chem. B* **2002**, *106* (40), 10388−10394.
(17) Ciccotti, G.; Ferrario, M.; Hynes, J. T.; Kapral, R. Dynamics of ion-pair interconversion in a polar-solvent. *J. Chem. Phys.* **1990**, *93* (10), 7137−7147.
(18) Ciccotti, G.; Ferrario, M.; Hynes, J. T.; Kapral, R. Constrained molecular-dynamics and the mean potential for an ion-pair in a polar-solvent. *Chem. Phys.* **1989**, *129* (2), 241−251.
(19) Essmann, U.; Perera, L.; Berkowitz, M. L.; Darden, T.; Lee, H.; Pedersen, L. G. A smooth particle mesh Ewald method. *J. Chem. Phys.* **1995**, *103* (19), 8577−8593.
(20) Ryckaert, J. P.; Ciccotti, G.; Berendsen, H. J. C. Numerical-integration of cartesian equations of motion of a system with constraints − molecular-dynamics of *n*-alkanes. *J .Comp. Phys.* **1977**, *23* (3), 327−341.
(21) Guardia, E.; Rey, R.; Padro, J. A. Potential of mean force by constrained molecular-dynamics − A sodium-chloride ion-pair in water. *Chem. Phys.* **1991**, *155* (2), 187−195.
(22) Hynes, J. T. Chemical reaction dynamics in solution. *Annu. Rev. Phys. Chem.* **1985**, *36*, 573−597.
(23) Das, A. K.; Madhusoodanan, M.; Tembe, B. L. Dynamics of Na^+−Cl^-, Na^+−Na^+, and Cl^-−Cl^- ion pairs in dimethyl sulfoxide: Friction kernels and transmission coefficients. *J. Phys. Chem. A* **1997**, *101* (15), 2862−2872.
(24) Grote, R. F.; Hynes, J. T. The stable states picture of chemical-reactions. 2. Rate constants for condensed and gas-phase reaction models. *J. Chem. Phys.* **1980**, *73* (6), 2715−2732.
(25) Zichi, D. A.; Hynes, J. T. A dynamical theory of unimolecular ionic dissociation reactions in polar-solvents. *J. Chem. Phys.* **1988**, *88* (4), 2513−2525.
(26) Chandler, D. Statistical-mechanics of isomerization dynamics in liquids and transition-state approximation. *J. Chem. Phys.* **1978**, *68* (6), 2959−2970.
(27) Rey, R.; Guardia, E. Dynamic aspects of the Na^+−Cl^- ion-pair association in water. *J. Phys. Chem.* **1992**, *96* (11), 4712−4718.
(28) Laage, D.; Hynes, J. T. On the residence time for water in a solute hydration shell: Application to aqueous halide solutions. *J. Phys. Chem. B* **2008**, *112* (26), 7697−7701.
(29) Koneshan, S.; Rasaiah, J.; Lynden-Bell, R.; Lee, S. Solvent structure, dynamics, and ion mobility in aqueous solutions at 25° C. *J. Phys. Chem. B* **1998**, *102*, 4193−4204.
(30) Impey, R. W.; Madden, P. A.; McDonald, I. R. Hydration and mobility of ions in solutions. *J. Phys. Chem. B* **1983**, *87* (26), 5071−5083.